Some Results in Anderson Localization

Chen Jia and Ziqi Liu

January 5, 2021

Abstract

In this paper, we focus on two interesting phenomenons in Anderson localization model: phase transition and boundary localization. Under some conditions, the amplitude of quantum states may localize on the boundary. We simulate the boundary localization under various model parameters, and calculate its probability under certain conditions theoretically. The phase transition phenomenone occurs in multi-well potential. We reveal the relationship between the eigenmode degeneracy and the phase transition, and give a concrete method to calculate the value of transition point. Theoretical results are consistent with the simulation. unfinished...

1 Introduction

unfinished...

2 Anderson localization under different boundaries

Anderson localization can be modeled as follows.

$$-\triangle u + Vu = \lambda u \qquad x \in \Omega \tag{1}$$

The original domain $\Omega = [0,1]^d$ is a d-dimension unit square($d = 1, 2$). In 1-d case, it is divided into N smaller intervals, and $N \times N$ smaller squares in 2-d case. In each interval or square, the potential $V(x)$ is constant. Its value on each part is determined randomly between 0 and K. The eigenfunction $u(x)$ and eigenvalue λ represents the eigenmodes and energy levels of the Hamiltonian.

Boundary conditions (BC) of the model can be choosen as Dirichlet

$$u|_{\partial\Omega} = 0 \tag{2}$$

Neumann

$$\frac{\partial u}{\partial \mathbf{n}}|_{\partial\Omega} = 0 \tag{3}$$

Robin($h > 0$)

$$(\frac{\partial u}{\partial \mathbf{n}} + hu)|_{\partial\Omega} = 0 \tag{4}$$

or parabolic boundary condition.

Most works focus on Dirichlet boundary condition, but we would indicate that eigenmodes and eigenvalues may perform differently under different boundary conditions. As shown in Figure 1, under Dirichlet and Neumann BC, difference of eigenmode is obvious, but egienvalues not. For larger eigenvalues, difference of eigenmodes are much larger.

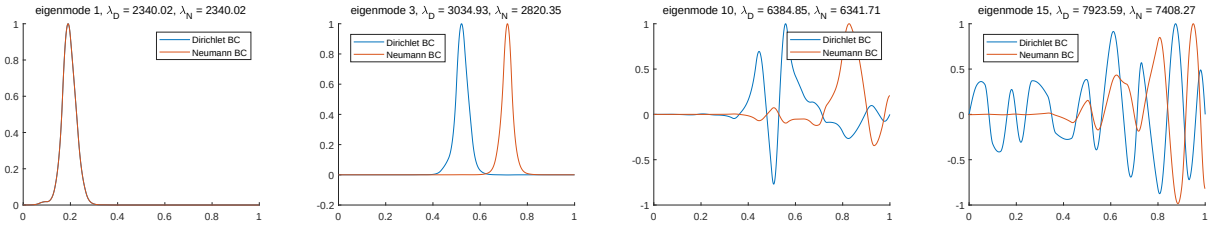

Figure 1: Eigenmodes and eigenvalues (1-d case) under Dirichlet BC (blue lines) and Neumann BC (red lines)

Figure 2 shows the 2-d case. It's intersting that both eigenvalues and eigenmodes are totally different in 2-d case.

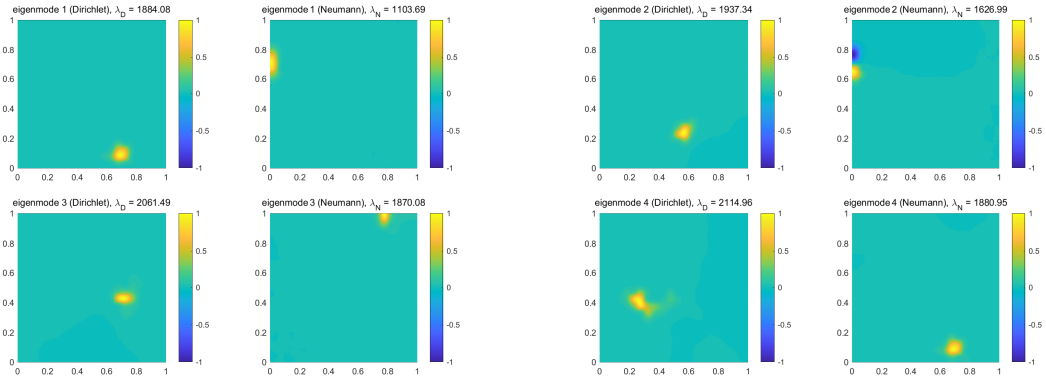

Figure 2: First 4 eigenmodes and eigenvalues (2-d case) under Dirichlet BC (left of each subfigure) and Neumann BC (right of each subfigure)

Eigenvalues under different boundary conditions performs differently in 1-d and 2-d case. Figure 3 shows the difference in respect of increasing rates.

We can see that under Dirichlet BC, eigenmodes can not localize to the boundary due to the enforce boundary condition, but under other boundary conditons, eigenmodes may localize to the boundary. It is one of mean results in this papper. Porbility of localization on boundary is discussed in Section 5.

boundary condition is important in model, our work make sense.

3 Landscape of localization

3.1 basic theroies

We compute the eigenmodes in 1-d case under different boundary conditions. Eigenmodes are normalized as $\|u\|_\infty = 1$. Random potential $V(x)$ and the eigenmodes $u(x)/\lambda$ (colored lines)

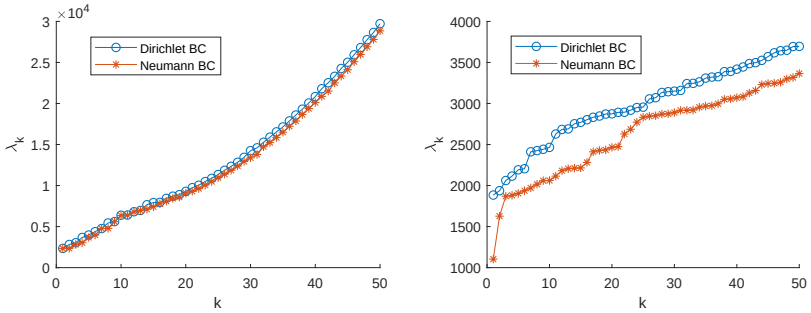

(a) 1-d case (b) 2-d case

Figure 3: Difference of eigenvalues between 1-d and 2-d case. x-axis represents the serial number k of eigenvalues and y-axis represents the correspoing eigenvalue λ_k

are shown in Figure 4. It seems diffcult for us to predict where the eigenmode will localize before simulation.

In order to predict where will eigenmodes localize, we introduce the landscape $w(x)$ as the sulotion of the right hand side equation with the same boundary condition.

$$-\triangle w + Vw = 1 \qquad x \in \Omega \tag{5}$$

In Figure 4, landscape is shown by black lines. Noting that eigenmodes and landscaps behave differently under different boundary conditions.

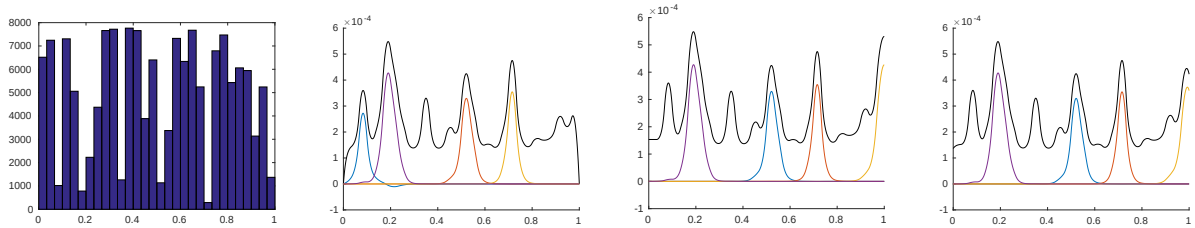

(a) potential (b) Dirichlet (c) Neumann (d) Robin

Figure 4: (a) The random potential $V(x)$ entering the equation(we choose $K = 5000$). The domain $[0, 1]$ is divided in $N = 30$ smaller intervals. (b-d) First 4 eigenmodes $u(x)/\lambda$ (colored lines) and landscape $w(x)$ (black line) under certian potential. eigenmodes and landscapes are computed under Dirichlet, Neumann, Robin ($h = 10$) BC.

In simulation, we can see that eigenmodes satisify $u(x)/\lambda \leq w(x)$, actually we have following therom.

Theorem 1 *Domain $\Omega \subset \mathbb{R}^d$ is an open bounded set. Consider $\lambda \in \mathbb{R}$ and $u(x)$ are one of the eigenvalue and corresponding eigenfunction of the second order elliptic problem*

$$-\nabla(A\nabla u) + b \cdot \nabla u + cu = \lambda u \qquad x \in \Omega \tag{6}$$

whose boundary condition can be Dirichlet, Neumann, Robin($h > 0$) and parabolic, $A(x)$ is positive define and $c(x) \leq 0$. $u(x)$ is normalized as $\|u\|_\infty = 1$.

Landscape $w(x)$ is the sulotion of this equation with the same boundary condition.

$$-\nabla(A\nabla w) + b \cdot \nabla w + cw = 1 \qquad x \in \Omega \tag{7}$$

Then we have

$$u(x) \leq \lambda\, w(x) \qquad x \in \Omega \tag{8}$$

Remark 1 *The idea of landscape first appeared in [1], but only the simplest case (Dirichlet BC + symetric operator) is strictly proofed. We expand the theory to the more general non-symetric operator and arbitrary boundries.*

3.2 valleylines and effective valleylines for 2-d case

When we come to 2-d case, landscape becomes more complex. We divied the peaks of landscape by valleylines which can be calculated by applying watershed algorithm to the reversed landscape. Along the valleylines, $w(x)$ is expected to be small. Valley lines divide the hole domain into many sub-domains, according to the therom 1, $u(x)$ is also small on the valleylines, so eigenmodes are likely to localize in these sub-domains.

Figure 5 shows the landscape, eigenmodes and valleylines under Neumann boundary condition. If we only consider the landscape in (b), we can hardly get the sketch of eigenmodes, but in (d), valleylines seperate the eigenmodes properly.

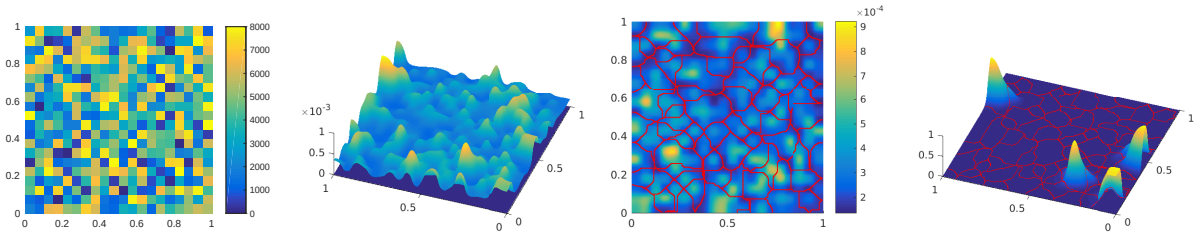

(a) potential (b) landscape (c) valleylines (d) eigenmodes

Figure 5: (a) The random potential $V(x)$ entering the equation($K = 8000$). The domain $[0, 1]^2$ is divided in 20×20 smaller squares. (b) 3-d view of landscape $w(x)$ under the potential and Neumann BC. (c) 2-d color representation of $w(x)$ and valleylines deduced from the landscape (red lines). (d) first 4 eigenmodes and valleylines.

For larger eigenvalues, since λ may be big, some parts of valleylines may lose their control on eigenmodes. That is, only the points on valleylines satisify $w(x) < 1$ is effective. We calculate larger eigenmodes and efective valleylines, shown in Figure 6. One can clearly observe that all modes are localized in one of the subregions divided by effective valleylines.

4 Limit Behavior under large K

In following sections, we consider the case that $V(x)$ in each interval or square corresponds Bernoulli distribution. That is, in each subdomain, potential is 0 with probability $1 - p$ and K with probability p.

In this case, we have the following therom.

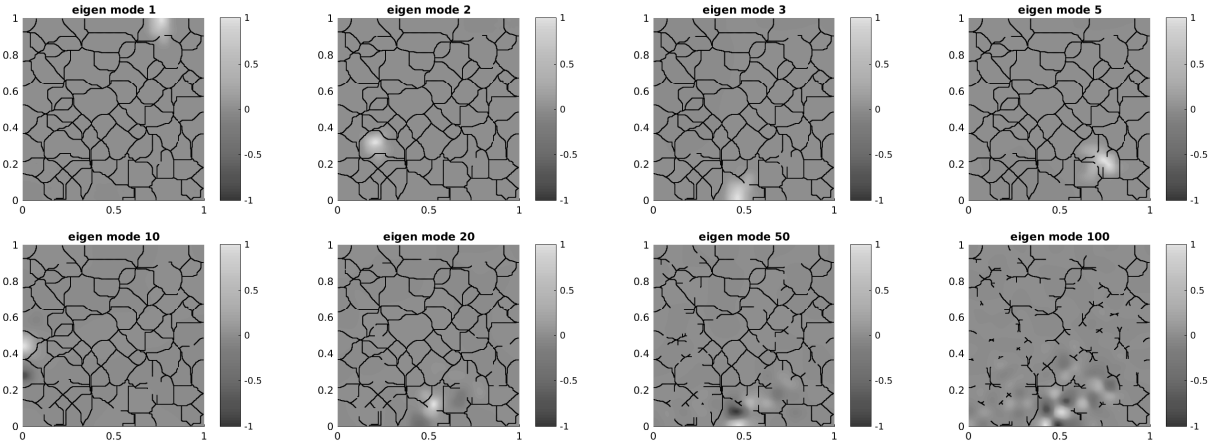

Figure 6: Eigenmodes and corresponding effecitve valleylines (black lines)

Theorem 2 *Domain $\Omega \subset \mathbb{R}^d$ is an open bounded set. Consider $\lambda \in \mathbb{R}$ and $u(x)$ are one of the eigenvalue and corresponding eigenfunction of the problem 1. $V(x) \in \{0, K\}$ $\forall\, x$ and $u(x)$ is normalized as $\|u\|_\infty = 1$.*

Then for the subdomian $D = \{x \in \Omega : V(x) = K\}$we have

$$\lim_{K\to\infty} u(x) = 0 \qquad \forall x \in D \tag{9}$$

According to the theorem, the original problem turns to some eigenvalue problems on subdomains where $V(x)$ is 0. The first eigenmode will licalize to the subdomain with smallest eigenvalue.

In 1-d case, the result is trival, we focous on the 2-d case. Figure 7 shows the potentials and valleylines for $p = 0.7$ with different K. With the increasing of K, the subdomains divided by valleylines split and finally coincides with the connected branches of $V(x) = 0$. Figure 8 shows the potentials and valleylines of $K = 10^4$, the valleylines surrounds the connected branch of $V(x) = 0$, and avoids crossing the parts of $V(x) = K$ as far as possible.

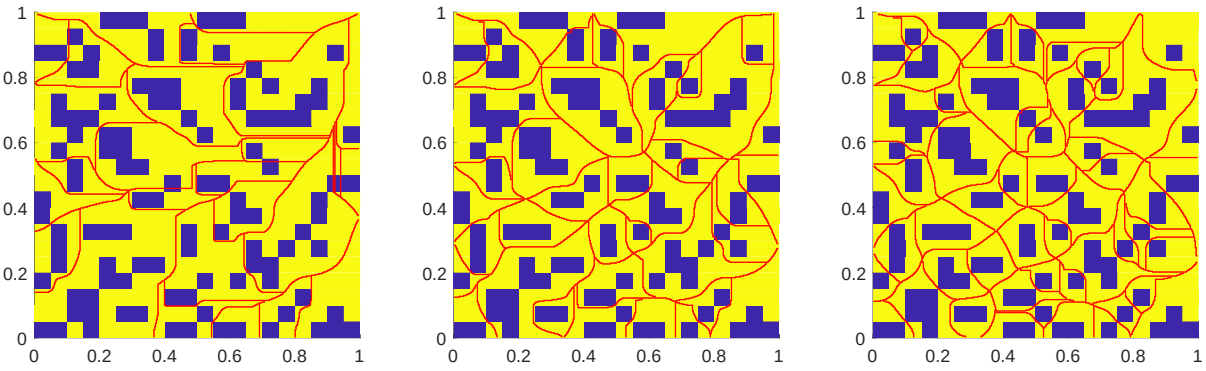

(a) $K = 10$ (b) $K = 100$ (c) $K = 1000$

Figure 7: Potentials (blue for $V(x) = 0$ and yellow for $V(x) = K$) and valleylines (red lines) for different K

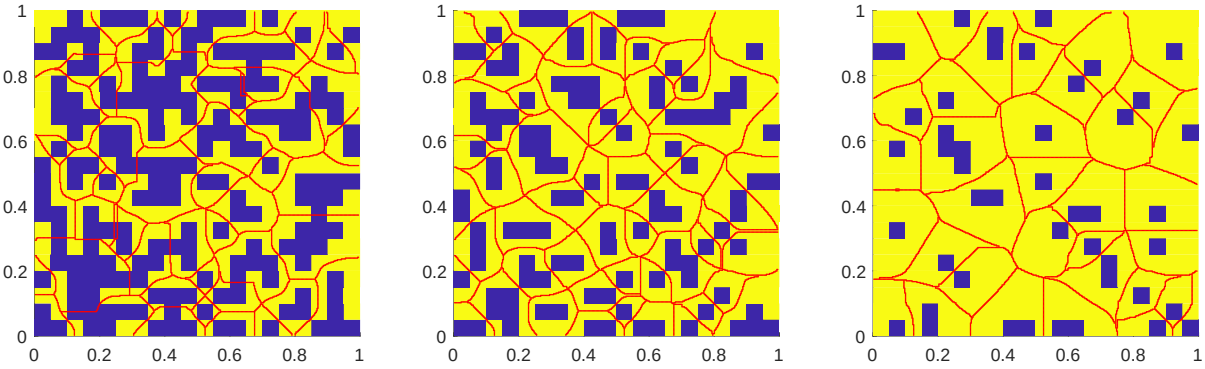

(a) $p = 0.5$ (b) $p = 0.7$ (c) $p = 0.9$

Figure 8: Potentials (blue for $V(x) = 0$ and yellow for $V(x) = K$) and valleylines (red lines) for $K = 10^4$

5 Localization to the boundary

In Section 3, we indicate that eigenmodes may localize to the boundary in Neumann and Robin BC. In this section, we will discuss the probability of localization to the boundary theoretically under specific conditions.

In the 1-d case, for a certain eigenmode, the degree of its localization to the boundary is defined as

$$P_b = \frac{\max\{|u(0)|, |u(1)|\}}{\max_{x\in\Omega} |u(x)|} \tag{10}$$

In 2-d case, we can define the degree of localization to the edge as

$$P_e = \frac{\max_{x\in\partial\Omega} |u(x)|}{\max_{x\in\Omega} |u(x)|} \tag{11}$$

and the degree of localization to the corner as

$$P_c = \frac{\max\{|u(0,0)|, |u(0,1)|, |u(1,1)|, |u(1,0)|\}}{\max_{x\in\Omega} |u(x)|} \tag{12}$$

Under Dirichlet BC, P_b, P_e and P_c are constantly 0, but under Neumann and Robin BC, these are random varaibles related on K, p and h. For simplicity, we focous on only the first eigenmode.

In following simulation, for 1-d case, hole domain $[0, 1]$ is divided into 50 small intervals, for 2-d case, $[0, 1]^2$ is divided into 15×15 small squares. We randomly generate the potential 1000 times to get the mean value of P_b, P_e and P_c.

5.1 some simulation results

relation of parameter h The degree of localization to the boundary varies to h with parameter $p = 0.5, K = 10^3$ is shown in the Figure 9. In Robin BC, when h goes to infinity, the boundary approches Dirichlet, and when h goes to 0, the boundary approches Neumann.

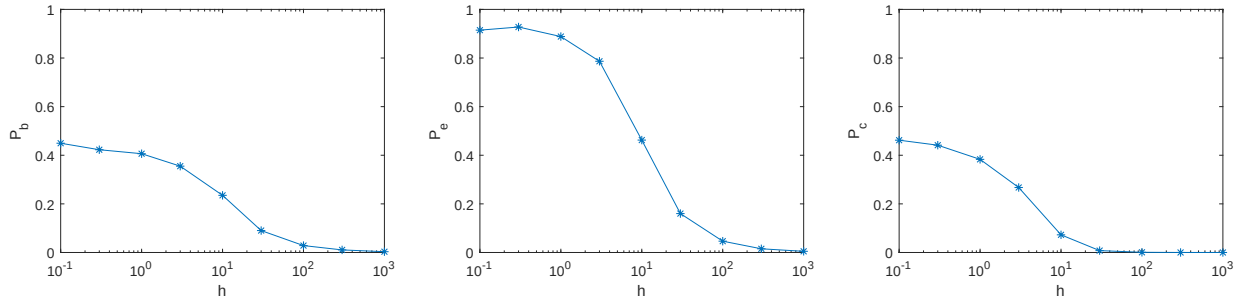

(a) boundary (b) edge (c) corner

Figure 9: The degree of localization to the boundary varies to h (parameter $p = 0.5, K = 10^3$)

relation of parameter p The degree of localization to the boundary varies to p with parameter $h = 1, K = 10^3$ is shown in the Figure 10. unfinished, how to explain this result?

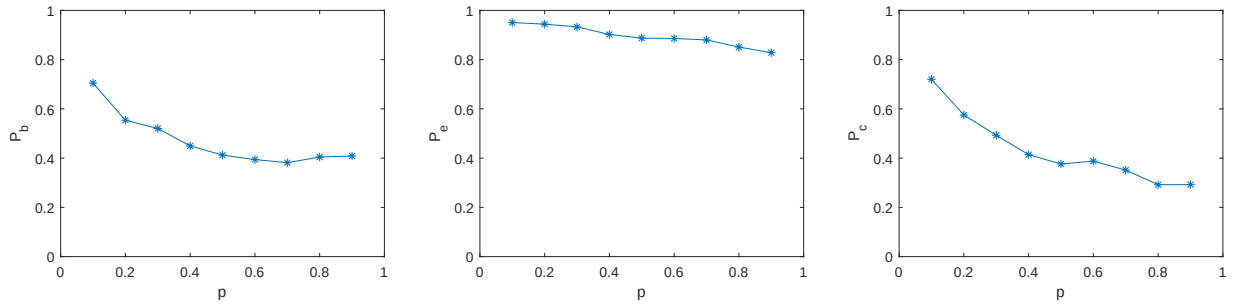

(a) boundary (b) edge (c) corner

Figure 10: The degree of localization to the boundary varies to p (parameter $h = 1, K = 10^3$)

relation of parameter K The degree of localization to the boundary varies to K with parameter $p = 0.5, h = 1$ is shown in the Figure 11. unfinished, how to explain this result?

5.2 A theoretical result for 1-d case

In 1-d case, for Dirhclet BC, the first eigenmode will localize to the longest interval on which $V(x) = 0$. Noting that there is some symmetric properties in Neumann BC. As shown in Figure 12, for an interval with left Neumann BC and right Dirichlet BC, the smallest eigenvalue is equal to the smallest eigenvalue on an interval with twice length and Dirichlet BC. Then we can get, if the longest extended subdomian is near the boundary, the first eigenmode will localize to the boundary.

As shown in Figure 13, we can also apply the theroy to 2-d case, in particular, the sub area near the corner will be extended twice. After extended, area of extended subdomains near the boundary become larger, that is for Neumann BC, eigenmodes are more likely localize to the boundary.

For sufficient big K and small h, the probability of "the first eigenmode localize to the boundary" is equal to the probability of the event that "the longest extended subdomain

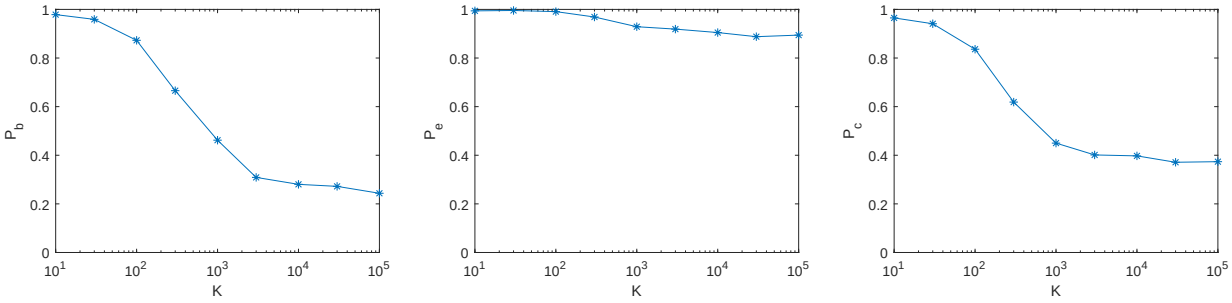

(a) boundary (b) edge (c) corner

Figure 11: The degree of localization to the boundary varies to K (parameter $p = 0.5, h = 1$)

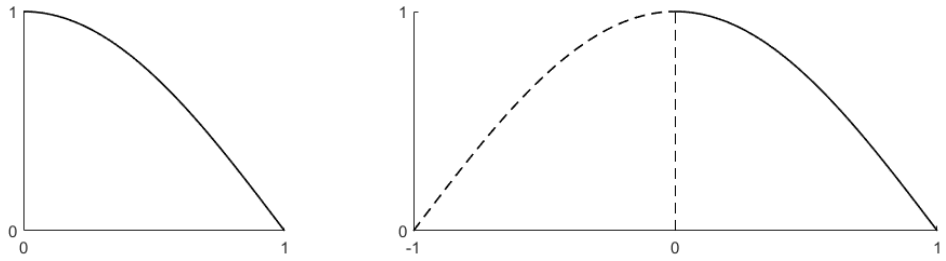

Figure 12: Extention for 1-d case

locates on the boundary". We can get its probability is

$$P_b = q^2p^2 \sum_{k=1}^{\infty} q^{k-2} \sum_{n=1}^{k-1} (1 - q^{2\max\{k-n,n\}-1})^{M-2} + pq^2 \sum_{n=1}^{\infty} (1 - p^{2n-1})^{M-2} p^{n-1} \tag{13}$$

Figure 14 show the simulation results and theoretical predictions. We choose parameters $K = 5 \times 10^4, h = 0.01$. The whole domain is divieded into $N = 50$ intervals. The theoretical prediction is in good agreement with the simulation.

6 Multimodality

Firstly, we introduce a simple example. Consider eigenmodes of pootential shown in Figure 15(a) with Dirichlet BC. Due to the symmetric properties of the potential, we have double eigenvalue $\lambda_1 = \lambda_2 = 211.5469$ and any linear combination ofeigenmode 1 and eigenmode 2 is also an eigenmmode.

Noting that both first and second eigenmodes have two peaks which called multimodality. From Figure 15(c) we can see, one can hardly get information of multimodality from the landscape. Landscape can only tell us where eigenmodes might localize, but can not describe the multimodality.

Multimodality may appear when the first eigenvalue is equal to the second. Recall the analysis in Section 5, for sufficient large K, the probability of multimodality is equal to the probability of "the longest two extended subdomain are the same length". For Dirichlet BC,

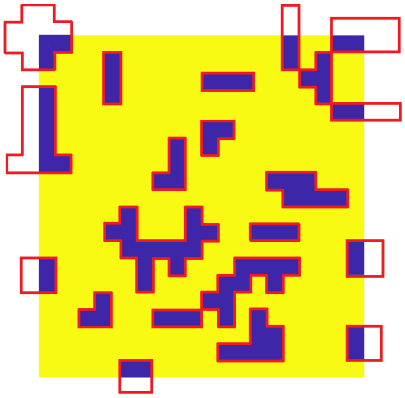

Figure 13: Extention in 2-d case. Blue for $V(x) = 0$ and yellow for $V(x) = K$. Effective subdomains are surronded by red lines.

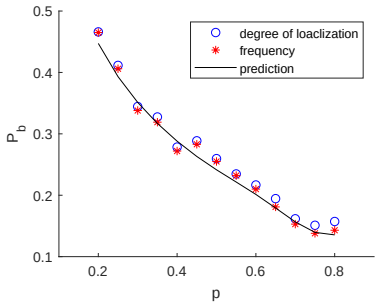

Figure 14: Simulation results and theoretical predictions for large K and small h. Blue circles represents the simulation result of P_b, red stars represents the frequency of the event "the longest extended subdomain locates on the boundary" in the simulation, black line represents the thoretical prediction of P_b for different p.

we can get its probability is

$$P_D = 1 - p\sum_{n=1}^{\infty}(1-p^{n-1})^{M-2}q^{n-1} \tag{14}$$

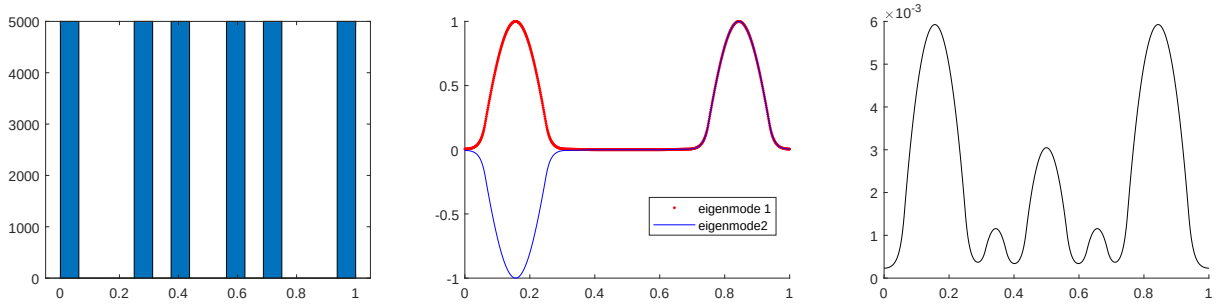

(a) potential (b) eigenmode (c) landscape

Figure 15: (a) The random potential $V(x)$ entering the equation($K = 8000$). (b) first 2 eigenmodes. (c) corresponding valleyline.

and for Neumann BC

$$\begin{aligned} P_N = 1 &- q^2(M-2)\sum_{n=1}^{\infty}(1-q^{(n-1)/2})^2(1-q^{n-1})^{M-3}q^{n-1}p \\ &- 2q^2\sum_{n=1}^{\infty}(1-q^{2n-1})^{M-2}(1-q^{n-1})q^{n-1}p \\ &- 2pq(M-1)\sum_{n=1}^{\infty}(1-q^{(n-1)/2})(1-q^{n-1})^{M-2}q^{n-1}p \\ &- 2pq\sum_{n=1}^{\infty}(1-q^{2n-1})^{M-1}q^{n-1}p \\ &- p^2M\sum_{n=1}^{\infty}(1-p^{n-1})^{M-1}q^{n-1}p \end{aligned} \tag{15}$$

Affected by calculation error, we can hardly observe that eigenvalues are exactly equal in practice, so we think that the multimodellity appears when the relative error between the first and the second eigenvalue satisity $\frac{\lambda_2-\lambda_1}{\lambda_1} < 0.02$.

Figure 16 show the simulation results and theoretical predictions. We choose parameters $K = 3 \times 10^6$. The whole domain is divieded into $N = 50$ intervals. The theoretical prediction is in good agreement with the simulation.

7 Phase transition

Consider 1-d case with parabolic BC, potietial is choosen as follows. As shown in Figure 17, in the whole domain $[0, 1]$, the values of potential are 0 and K alternately in the intervals with length $L_2/2, L_1, L_2, L_3, L_4, L_3, L_2/2$. We can consider the potential as two wells Ω_1, Ω_2 with length L_1 and $2L_3$, while there is a barrier with length L_4 in the middle of the second well.

In the potential, L_2 is big enough to seprate two wells and L_4 is small. For detials, potential must satisify: $L_3 < L_1 < 2L_3$ (two wells are about the same length), $L_4 < L_3/2$ (barrier should be short enough), $L_2 > L_1 + L_3 + L_4 + L_3$ (L_2 should be big enough to seperate the two wells), and total length $L_1 + 2L_2 + 2L_3 + L_4 = 1$.

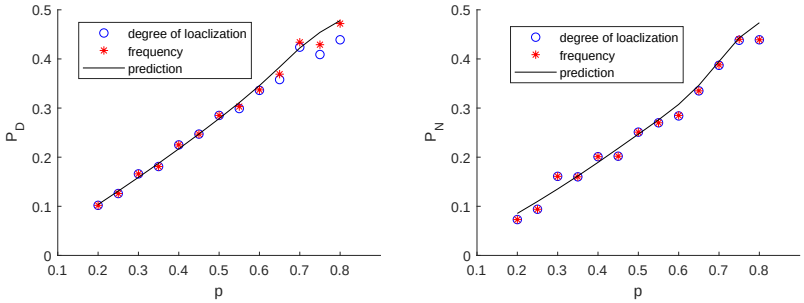

(a) Dirichlet BC (b) Neumann BC

Figure 16: Simulation results and theoretical predictions for large K. Blue circles represents the simulation result of P_D and P_N, red stars represents the frequency of the event in the simulation, black lines represents the thoretical prediction of P_D and P_N for different p.

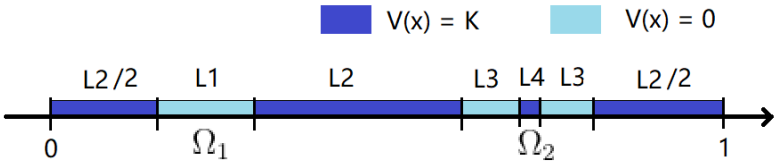

Figure 17: A diagram of potential $V(x)$

Since the second well is longer, when K is small, barrier is not strong enough, so the first eigenmode will localize to the second well. But when K is big, the first eigenmode will localize to the first well. For increasing K, eigenmode will jump from the second well to the first, which is called phase transition.

We choose $L_1 = 1/12, L_2 = 2/5, L_3 = 1/20, L_4 = 1/60$. The first two eigenmodes and landscapes for different K is shown in Figure 18. One can see that for different K, landscapes are almost same, but the eigenmodes changes a lot.

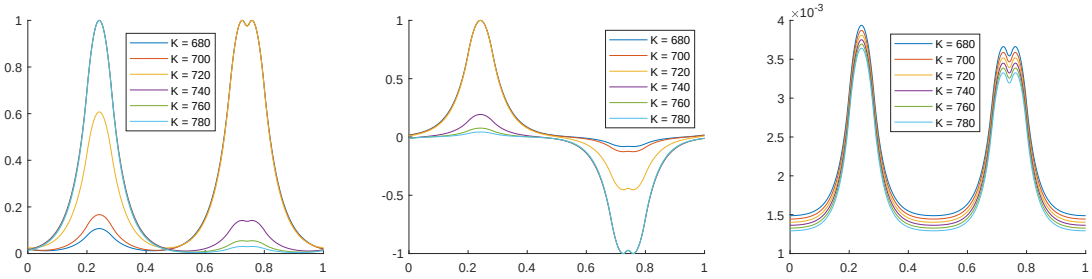

(a) eigenmode 1 (b) eigenmode 2 (c) landscape

Figure 18: The first two eigenmodes and landscapes for different K

Eigenmodes and landscapes may appear two peakes in Ω_1 and Ω_2. For a certain function $u(x)$, we define the relative height of the left peak F as

$$F = \frac{\max_{x\in\Omega_1} |u(x)|}{\max_{x\in\Omega_1} |u(x)| + \max_{x\in\Omega_2} |u(x)|} \tag{16}$$

Relative height of left peak in eigenmodes and landscapes are shown in Figure 19 (a-c). one can see that the relative heigth of peak of landscape is approximately constant for different K but eigenmodes appears phase transition. We define the K satisify the left and right peak of the first eigenmode is equal in height as the critical point K_c in phase transition.

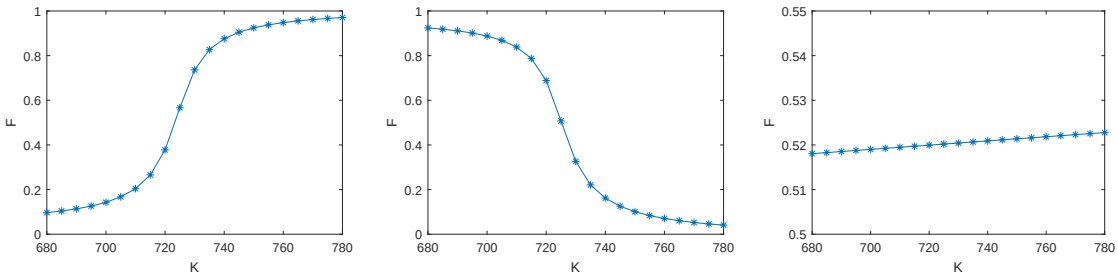

(a) eigenmode 1 (b) eigenmode 2 (c) landscape

Figure 19: Relative heights of peaks in eigenmodes and landscape various with parameter K.

Figure 21 (b) shows the variation of the first and second eigenvalue with K. In this problem, the potential has two wells. So we can divide the problem into two subsystems. The eigenmode localized to the left corresponds to an subsystem, and the eigenmode localized to the left corresponds to another.

As shown in Figure 20, set the value in Ω_1 to K and we can get $V_1(x)$. Similiarly, set the value in Ω_2 to K and we can get $V_2(x)$. The system into two subsystems with potential $V_1(x)$ and $V_2(x)$.

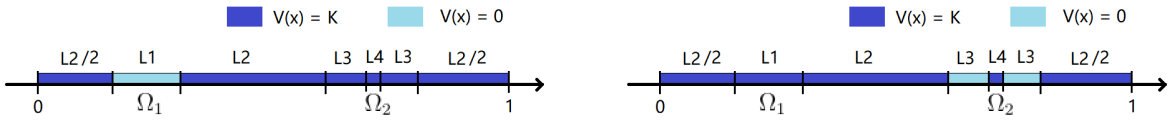

(a) $V_1(x)$ (b) $V_2(x)$

Figure 20: A diagram of potential $V_1(x)$ and $V_2(x)$ in subsystems.

We choose $L_1 = 1/12, L_2 = 2/5, L_3 = 1/20, L_4 = 1/60$, the eigenmodes and eigenvalues of subsystems are shown in Figure 21. From Figure 21 (a) we can see that eigenmodes of subsystems are almost same with the eigenmodes of the original problem. Figure 21 shows the eigenvalues for different K. Both the first eigenvalues increase with the increase of K, but they increase at different rates. When one eigenvalue is equal to the other, the minimum eigenvalue changes from one to the other, then the phase transition occurs.

We can proof that for parameter K, the first eigenvalue of subsystem on Ω_1 satisify the equation

$$0 = D_1(K, \lambda) = \alpha \tan(\alpha x_0) - \beta \tanh(\beta(\frac{1}{2} - x_0)) \tag{17}$$

where $\alpha = \sqrt{\lambda}, \beta = \sqrt{K - \lambda}, x_0 = L_1/2$.

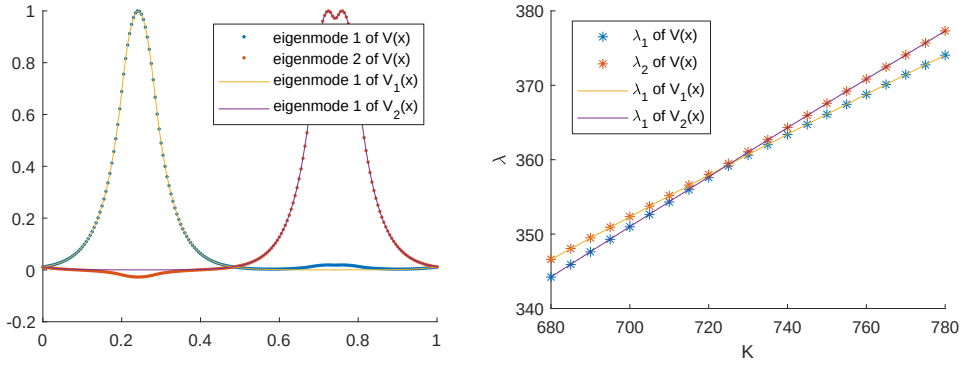

(a) eigenmodes (b) eigenvalues

Figure 21: Eigenmodes and eigenvalues of subsystems

Similarly, the first eigenvalue of subsystem on Ω_1 satisify the equation

$$\begin{aligned} 0 = D_2(K,\lambda) =&(\alpha^2-\beta^2)(\mathrm{e}^{2\beta x_2}+\mathrm{e}^{2\beta(x_1+x_3)})/(\mathrm{e}^{2\beta(x_1+x_3)}-\mathrm{e}^{2\beta x_2}) \\ &+(\alpha^2+\beta^2)(\mathrm{e}^{2\beta x_3}+\mathrm{e}^{2\beta(x_1+x_2)})/(\mathrm{e}^{2\beta(x_1+x_3)}-\mathrm{e}^{2\beta x_2}) \\ &+2\alpha\beta\cot(\alpha(x_1-x_2)) \end{aligned} \tag{18}$$

where $x_1 = L_4/2, x_2 = L_4/2 + L_3, x_3 = 1/2$.

When pahse transition occurs, eigenvalue in both subsystem are equal, so the citical point K_c and the ciritcal eigenvalue λ_c satisify

$$D_1(K_c,\lambda_c) = 0 \tag{19}$$
$$D_2(K_c,\lambda_c) = 0 \tag{20}$$

We generate L_1, L_2, L_3, L_4 randomly, Firgure 22 shows the prediction from 19 and the simulation results, we can see that the prediction is accurate.

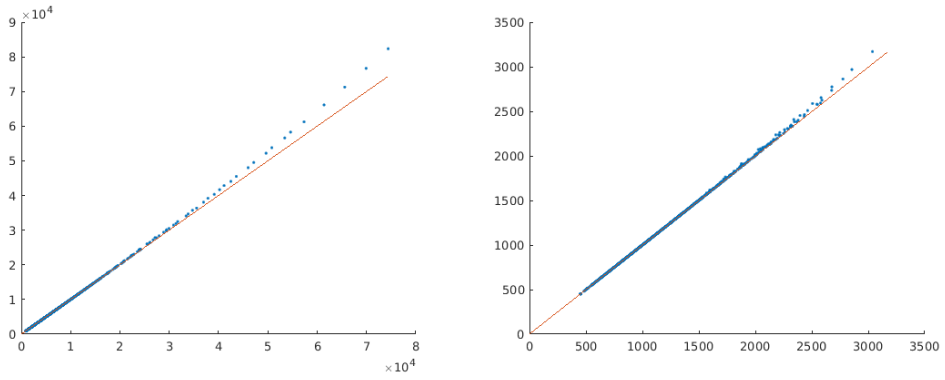

(a) K_c (b) λ_c

Figure 22: simulation and prediction results. x-axis reresents the prediction value and y-axis represents the simulation results. Each blue point represents a random sample and the red line is $x = y$.

8 Couclusion

unfinished...

A Proof of landscape theorem 1

Define the second order elliptic operator

$$\mathcal{L}u = -\nabla(A\nabla u) + b \cdot \nabla u + cu$$

then λ, $u(x)$ and $w(x)$ satisify

$$\mathcal{L}u = \lambda u \qquad \mathcal{L}(\lambda w) = \lambda$$

Noting that $u(x)$ can be seen as the solution of

$$\mathcal{L}u = g$$

where $g(x) = \lambda u(x)$. Since $\|u\|_\infty = 1$, we have $g(x) \leq \lambda$.

According to the maximum principle, we can get

$$u(x) \leq \lambda\, w(x) \qquad x \in \Omega$$

B Proof of theorem 2

unfinished...

C Geometric distributation approximation

Accordong to the symmetric in Nuemann BC, for sufficient big K, the probability of "the first eigenmode localize to the boundary" is equal to the probability of the event that "twice of the length of a segment with value of 0 on the boundary is larger than all of segments with value of 0 inside".

Suppose that the previous two intervals with the value of 1 and 0, let the number of following intervals with the value of 0 be X, then X is a random variable. For a sufficient large N, X approximately obeys the geometric distribution with parameter p.

$$\mathbb{P}(X = n) = q^{n-1}p$$

thus

$$\mathbb{P}(X < n) = 1 - q^{n-1}$$

where $q = 1 - p$.

Similarly, length of continuous intervals with of value 1 is a random variable with probability

$$\mathbb{P}(Y = n) = p^{n-1}q$$

In the whole interval, X and Y must appear alternately. The average length of each period is $E(X + Y) = \frac{1}{pq}$. So the average number of periods in the whole domain is $M = Npq$. In the average sense, we can approximately regard the whole domain consists of intervals with length $X_1, Y_1, \cdots, X_M, Y_M$. For a sufficient large N, random variables $X_1, Y_1, \cdots, X_M, Y_M$ are approximately independent.

C.1 Callculation of equation 13

The event "localize to the boundary" can be splitted into the following situations:

situation 1 $V(0) = V(1) = 0$ with probability q^2.

Under such conditions, we have

$$\begin{aligned}
&\mathbb{P}(\max\{X_2, X_3, \cdots, X_{M-1}\} < 2\max\{X_1, X_M\}) \\
=&\sum_{m,n=1}^{\infty} \mathbb{P}(\max\{X_2, X_3, \cdots, X_{M-1}\} < 2\max\{m, n\})\mathbb{P}(X_1 = m)\mathbb{P}(X_M = n) \\
=&\sum_{m,n=1}^{\infty} [\mathbb{P}(X_k < 2\max\{m, n\})]^{M-2}\mathbb{P}(X_1 = m)\mathbb{P}(X_M = n) \\
=&\sum_{m,n=1}^{\infty} (1 - q^{2\max\{m,n\}-1})^{M-2} q^{m-1} p q^{n-1} p \\
=&\sum_{k=1}^{\infty} q^{k-2} p^2 \sum_{n=1}^{k-1} (1 - q^{2\max\{k-n,n\}-1})^{M-2}
\end{aligned}$$

situation 2 $V(0) = 0, V(1) = 1$ with probability pq.

Under such conditions, we have

$$\begin{aligned}
&\mathbb{P}(\max\{X_2, X_3, \cdots, X_M\} < 2X_1) \\
=&\sum_{n=1}^{\infty} \mathbb{P}(\max\{X_2, X_3, \cdots, X_{M-1}\} < 2n)\mathbb{P}(X_1 = n) \\
=&\sum_{n=1}^{\infty} [\mathbb{P}(X_k < 2n)]^{M-1}\mathbb{P}(X_1 = n) \\
=&q\sum_{n=1}^{\infty} (1 - p^{2n-1})^{M-2} p^{n-1}
\end{aligned}$$

situation 3 $V(0) = 1, V(1) = 0$ with probability pq, which can be calculated simillary to situation 2.

In summary, probability of localize to the boundary is

$$q^2 p^2 \sum_{k=1}^{\infty} q^{k-2} \sum_{n=1}^{k-1} (1 - q^{2\max\{k-n,n\}-1})^{M-2} + pq^2 \sum_{n=1}^{\infty} (1 - p^{2n-1})^{M-2} p^{n-1}$$

C.2 Calculation of equation 14

For Dirichlet Boundary, probability of "there is a unique longest subdomain with $V(x) = 0$" is

$$\begin{aligned}
&\sum_{k=1}^{M} \mathbb{P}(\max\{X_1, X_2, \cdots, X_{k-1}, X_{k+1}, \cdots, X_M\} < X_k) \\
=&M\ \mathbb{P}(\max\{X_2, X_3, \cdots, X_M\} < X_1) \\
=&M \sum_{n=1}^{\infty} \mathbb{P}(\max\{X_2, X_3, \cdots, X_{M-1}\} < n)\mathbb{P}(X_1 = n) \\
=&M \sum_{n=1}^{\infty} [\mathbb{P}(X_k < n)]^{M-1}\mathbb{P}(X_1 = n) \\
=&M \sum_{n=1}^{\infty} (1 - p^{n-1})^{M-1} q^{n-1} p
\end{aligned}$$

C.3 Calculation of equation 15

For Neumann Boundary, probability of "there is a unique longest extended subdomain with $V(x) = 0$" can be splitted into the following situations:

situation 1 $V(0) = V(1) = 0$ with probability q^2.

Under such conditions, we have

$$\begin{aligned}
&\sum_{k=2}^{M-1}\mathbb{P}(\max\{2X_1,X_2,\cdots,X_{k-1},X_{k+1},\cdots,2X_M\}<X_k)\\
&+\mathbb{P}(\max\{X_2,\cdots,X_{M-1},2X_M\}<2X_1)\\
&+\mathbb{P}(\max\{2X_1,X_2,\cdots,X_{M-1}\}<2X_M)\\
&=(M-2)\mathbb{P}(\max\{2X_1,X_3\cdots,2X_M\}<X_2)\\
&+2\mathbb{P}(\max\{X_2,\cdots,X_{M-1},2X_M\}<2X_1)\\
&=(M-2)\sum_{n=1}^{\infty}\mathbb{P}(\max\{2X_1,X_3\cdots,2X_M\}<n)\mathbb{P}(X_2=n)\\
&+2\sum_{n=1}^{\infty}\mathbb{P}(\max\{X_2,\cdots,X_{M-1},2X_M\}<2n)\mathbb{P}(X_1=n)\\
&=(M-2)\sum_{n=1}^{\infty}[\mathbb{P}(2X_k<n)]^2[\mathbb{P}(X_k<n)]^{M-3}\mathbb{P}(X_2=n)\\
&+2\sum_{n=1}^{\infty}[\mathbb{P}(X_k<2n)]^{M-2}\mathbb{P}(X_k<n)\mathbb{P}(X_1=n)\\
&=(M-2)\sum_{n=1}^{\infty}(1-q^{(n-1)/2})^2(1-q^{n-1})^{M-3}q^{n-1}p\\
&+2\sum_{n=1}^{\infty}(1-q^{2n-1})^{M-2}(1-q^{n-1})q^{n-1}p
\end{aligned}$$

situation 2 $V(0)=0, V(1)=1$ with probability pq.

Under such conditions, we have

$$\begin{aligned}
&\sum_{k=2}^{M}\mathbb{P}(\max\{2X_1,X_2,\cdots,X_{k-1},X_{k+1},\cdots,X_M\}<X_k)\\
&+\mathbb{P}(\max\{X_2,\cdots,X_{M-1},X_M\}<2X_1)\\
&=(M-1)\mathbb{P}(\max\{2X_1,X_3\cdots,X_M\}<X_2)\\
&+\mathbb{P}(\max\{X_2,\cdots,X_{M-1},X_M\}<2X_1)\\
&=(M-1)\sum_{n=1}^{\infty}\mathbb{P}(\max\{2X_1,X_3\cdots,X_M\}<n)\mathbb{P}(X_2=n)\\
&+\sum_{n=1}^{\infty}\mathbb{P}(\max\{X_2,\cdots,X_{M-1},X_M\}<2n)\mathbb{P}(X_1=n)\\
&=(M-1)\sum_{n=1}^{\infty}\mathbb{P}(2X_k<n)[\mathbb{P}(X_k<n)]^{M-2}\mathbb{P}(X_2=n)\\
&+\sum_{n=1}^{\infty}[\mathbb{P}(X_k<2n)]^{M-1}\mathbb{P}(X_1=n)\\
&=(M-1)\sum_{n=1}^{\infty}(1-q^{(n-1)/2})(1-q^{n-1})^{M-2}q^{n-1}p\\
&+\sum_{n=1}^{\infty}(1-q^{2n-1})^{M-1}q^{n-1}p
\end{aligned}$$

situation 3 $V(0)=1,V(1)=0$ with probability pq, which can be calculated simillary to situation 2.

situation 4 $V(0)=1,V(1)=1$ with probability p^2, which can be calculated simillary to Dirichlet BC.

In summary, probability of multimodellity on Neumann BC is

$$\begin{aligned}
P_N=1&-q^2(M-1)\sum_{n=1}^{\infty}(1-q^{(n-1)/2})(1-q^{n-1})^{M-2}q^{n-1}p\\
&-2q^2\sum_{n=1}^{\infty}(1-q^{2n-1})^{M-1}q^{n-1}p\\
&-2pq(M-1)\sum_{n=1}^{\infty}(1-q^{(n-1)/2})(1-q^{n-1})^{M-2}q^{n-1}p\\
&-2pq\sum_{n=1}^{\infty}(1-q^{2n-1})^{M-1}q^{n-1}p\\
&-p^2M\sum_{n=1}^{\infty}(1-p^{n-1})^{M-1}q^{n-1}p
\end{aligned}$$

D Calculation of equation 17 and 18

As shown in the Figure 23, we can transform the problem into eigenvalue problem on a half interval with Neumann BC.

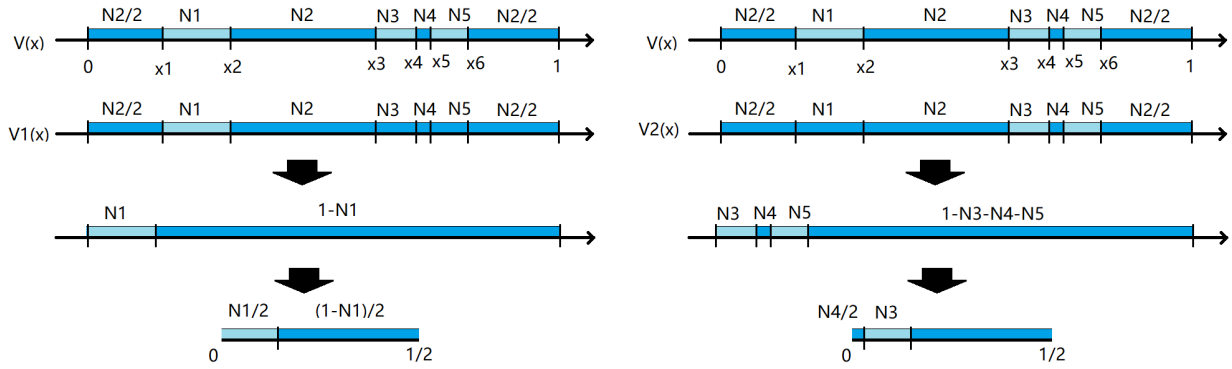

Figure 23: A diagram of potential $V(x)$

subsystem on Ω_1

We can regard it as a problem with Neumann BC in $[0, 1/2]$. In the interval $[0, x_0]$, $V(x)$ takes the value K and in $[x_0, 1/2]$ takes 0, where $x_0 = L_1/2$.

We define $\alpha = \sqrt{\lambda}, \beta = \sqrt{K - \lambda}$. in the interval $[0, x_0]$, the eigenmode can be written as

$$u(x) = A\sin(\alpha x) + B\cos(\alpha x) \qquad u'(x) = A\alpha\cos(\alpha x) - B\alpha\sin(\alpha x)$$

and in the interval $[x_0, 1/2]$,

$$u(x) = C\exp(\beta x) + D\exp(-\beta x) \qquad u'(x) = C\beta\exp(\beta x) - D\beta\exp(-\beta x)$$

where A, B, C, D are the parameter to be determined.

According to the Neumann BC and continuity, we have

$$\begin{aligned} u'(0) &= A\alpha = 0 \\ u'(1/2) &= C\beta\exp(\beta/2) - D\beta\exp(-\beta/2) = 0 \\ u(x_0) &= A\sin(\alpha x_0) + B\cos(\alpha x_0) = C\exp(\beta x_0) + D\exp(-\beta x_0) \\ u'(x_0) &= A\alpha\cos(\alpha x_0) - B\alpha\sin(\alpha x_0) = C\beta\exp(\beta x_0) - D\beta\exp(-\beta x_0) \end{aligned}$$

that is

$$\begin{bmatrix} \alpha & 0 & 0 & 0 \\ 0 & 0 & \beta e^{\frac{\beta}{2}} & -\beta e^{-\frac{\beta}{2}} \\ \sin(\alpha x_0) & \cos(\alpha x_0) & -e^{\beta x_0} & -e^{-\beta x_0} \\ \alpha\cos(\alpha x_0) & -\alpha\sin(\alpha x_0) & -\beta e^{\beta x_0} & \beta e^{-\beta x_0} \end{bmatrix} \begin{bmatrix} A \\ B \\ C \\ D \end{bmatrix} = \begin{bmatrix} 0 \\ 0 \\ 0 \\ 0 \end{bmatrix}$$

The existence of solutions is equivalent to

$$\det(A) = \alpha e^{2\beta x_0}\sin(\alpha x_0) - \beta e^{\beta}\cos(\alpha x_0) + \alpha e^{\beta}\sin(\alpha x_0) + \beta e^{2\beta x_0}\cos(\alpha x_0) = 0$$

that is

$$D_1(K, \lambda) = \alpha\tan(\alpha x_0) - \beta\tanh(\beta(\frac{1}{2} - x_0)) = 0$$

subsystem on Ω_2

We can regard it as a problem with Neumann BC in $[0, 1/2]$. In the interval $[0, x_1]$ and $[x_2, 1/2]$, $V(x)$ takes the value K and in $[x_1, x_2]$ takes 0. Where $x_1 = L_4/2, x_2 = N_4/2 + N_3$.

In the interval $[0, x_0]$, the eigenmode can be written as

$$u(x) = A\exp(\beta x) + B\exp(-\beta x) \qquad u'(x) = A\beta\exp(\beta x) - B\beta\exp(-\beta x)$$

and in the interval $[x_1, x_2]$,

$$u(x) = C\sin(\alpha x) + D\cos(\alpha x) \qquad u'(x) = C\alpha\cos(\alpha x) - D\alpha\sin(\alpha x)$$

and in the interval $[x_2, 1/2]$,

$$u(x) = E\exp(\beta x) + F\exp(-\beta x) \qquad u'(x) = E\beta\exp(\beta x) - F\beta\exp(-\beta x)$$

where A, B, C, D, E, F are the parameter to be determined.

According to the Neumann BC and continuity, we have

$$\begin{aligned}
u'(0) &= A\beta - B\beta = 0 \\
u(x_1) &= A\exp(\beta x_1) + B\exp(-\beta x_1) = C\sin(\alpha x_1) + D\cos(\alpha x_1) \\
u'(x_1) &= A\beta\exp(\beta x_1) - B\beta\exp(-\beta x_1) = C\alpha\cos(\alpha x_1) - D\alpha\sin(\alpha x_1) \\
u(x_2) &= C\sin(\alpha x_2) + D\cos(\alpha x_2) = E\exp(\beta x_2) + F\exp(-\beta x_2) \\
u'(x_2) &= C\alpha\cos(\alpha x_2) - D\alpha\sin(\alpha x_2) = E\beta\exp(\beta x_2) - F\beta\exp(-\beta x_2) \\
u'(1/2) &= E\beta\exp(\beta/2) - F\beta\exp(-\beta/2) = 0
\end{aligned}$$

that is

$$\begin{bmatrix}
1 & -1 & 0 & 0 & 0 & 0 \\
\mathrm{e}^{\beta x_1} & \mathrm{e}^{-\beta x_1} & -\sin(\alpha x_1) & -\cos(\alpha x_1) & 0 & 0 \\
\beta\mathrm{e}^{\beta x_1} & -\beta\mathrm{e}^{-\beta x_1} & -\alpha\cos(\alpha x_1) & \alpha\sin(\alpha x_1) & 0 & 0 \\
0 & 0 & \sin(\alpha x_2) & \cos(\alpha x_2) & -\mathrm{e}^{\beta x_2} & -\mathrm{e}^{-\beta x_2} \\
0 & 0 & \alpha\cos(\alpha x_2) & -\alpha\sin(\alpha x_2) & -\beta\mathrm{e}^{\beta x_2} & \beta\mathrm{e}^{-\beta x_2} \\
0 & 0 & 0 & 0 & \mathrm{e}^{\frac{\beta}{2}} & -\mathrm{e}^{-\frac{\beta}{2}}
\end{bmatrix}$$

The existence of solutions is equivalent to

$$\begin{aligned}
&\alpha^2\mathrm{e}^{2\beta(x_1+x_2)} + \alpha^2\mathrm{e}^{2\beta(x_1+x_3)} \\
&+\beta^2\mathrm{e}^{2\beta(x_1+x_2)} - \beta^2\mathrm{e}^{2\beta(x_1+x_3)} \\
&+\alpha^2\mathrm{e}^{2\beta x_2} + \alpha^2\mathrm{e}^{2\beta x_3} \\
&-\beta^2\mathrm{e}^{2\beta x_2} + \beta^2\mathrm{e}^{2\beta x_3} \\
&+2\alpha\beta\mathrm{e}^{2\beta(x_1+x_3)}\cot(\alpha(x_1-x_2)) - 2\alpha\beta\mathrm{e}^{2\beta x_2}\cot(\alpha(x_1-x_2)) = 0
\end{aligned}$$

that is

$$\begin{aligned}
0 = D_2(K,\lambda) =&(\alpha^2-\beta^2)(\mathrm{e}^{2\beta x_2} + \mathrm{e}^{2\beta(x_1+x_3)})/(\mathrm{e}^{2\beta(x_1+x_3)} - \mathrm{e}^{2\beta x_2}) \\
&+(\alpha^2+\beta^2)(\mathrm{e}^{2\beta x_3} + \mathrm{e}^{2\beta(x_1+x_2)})/(\mathrm{e}^{2\beta(x_1+x_3)} - \mathrm{e}^{2\beta x_2}) \\
&+2\alpha\beta\cot(\alpha(x_1-x_2))
\end{aligned}$$

where $x_3 = \frac{1}{2}$.

References

[1] M. Filoche and S. Mayboroda. Universal mechanism for Anderson and weak localization, PNAS. vol. 109, no. 37, 14761–14766